

# Flettner-rotor-powered VTOL's theoretical performances

Satoki Shimamune\*

*University of Cambridge, Cambridge, CB21TP, U.K.*

Dr Dmitry Ignatyev†

*Cranfield University, Cranfield MK430AL, U.K.*

**The demand for VTOLs is growing rapidly. From inspection to logistics, thanks to the evolution of autonomous technology. However, most of the fields remain just possibilities rather than actual usage cases due to the limited flight range, wall interaction, noise and instability of the aircraft. Alleviating an instability is especially an important key to achieve a reliable aerial system. One reason of instability is due to the limited four degrees of freedom. (i.e. VTOLs have to tilt to move horizontally) In this paper, a Flettner-force-powered VTOL that has six degrees of freedom, called Horizonist, is proposed and the stability of Horizonist is discussed in comparison to the conventional. (Horizonist is filed as a patent in Japan (issued as JP6938005) and PCT) The performances are evaluated in terms of settling time and power consumption against various inputs and a wind.**

## I. Nomenclature

$A$	=	area of the Flettner rotor
$w$	=	width of an aircraft
$C_m$	=	moment coefficient
$C_D$	=	lateral drag coefficient of an aircraft
$C_L$	=	force coefficient of the Flettner rotor
$dt$	=	time step
$F_{magnus}$	=	force created by the Flettner rotor
$F_{magnus_y}$	=	y component of $F_{magnus}$
$T_{magnus}$	=	Anti-torque created by the Flettner rotor
$T$	=	Torque created by the actuators, i.e. rotors
$T_{max}$	=	Maximum torque that can be generated by the aircraft
$Re$	=	Reynolds Number
$h$	=	height
$g$	=	gravitational acceleration assumed to be $9.81\text{kg}/\text{m}^2$
$\rho$	=	density of the air, assumed to be constant and $1.2\text{kg}/\text{m}^3$

## II. Introduction

The Flettner-rotor-powered VTOL aircraft that is covered in this paper allows the aircraft to move horizontally without tilting its body or any actuators. The physics is almost the same as Flettner airplanes [1]. As shown in Figure 1, Horizonist has a rotating surface arm [142a] in Figure 1, powered by an actuator [144a] in Figure 1, that is attached to a fixed arm [130a] in Figure 1, in addition to normal VTOL architectures. The aircraft's arms are doubled layered, and inner layer is fixed. However, outer layer [142a] is rotatable, and is exposed to the down wash created by rotors [122a]. As such, thanks to the Magnus effect, the thrust is created horizontally, allowing the aircraft to move horizontally. In Figure 2, the relationship between rotating surface and downwash is described so that the reason why horizontal thrust can be generated is seen.  $\omega$  is the direction of the rotation of the rotating surface and force is generated rightward in Figure 2.

---

\*Undergraduate, St John's College, Department of Engineering, ss2759@cam.ac.uk

†Senior Research Fellow, School of Aerospace, Transport and Manufacturing

Compared to conventional VTOLs, the aircraft does not need to tilt to create horizontal thrust, and thus, the time and the energy taken to tilt the aircraft's body can be saved by the virtue of Flettner rotors on arms.

In addition to the main discussion about the stability and power consumption, Horizonist's high affinity with the conventional VTOL designs while maintaining flight mechanical independence from the conventional flight method is important to be noted. Horizonist only requires to add rotating the surface on the aircraft's arms' surface, so Flettner rotors does not affect the normal flight when idling. This leads to that even at the event of Horizonist's failure, in contrast to tilt rotors and electronically powered gimbals [2–4], the aircraft can safely maintain its normal flight thanks to its independence. The video of the prototype can be accessed via [https://drive.google.com/file/d/1abCoLPoN80W\\_N0xPl09FCbCky3hVVV0r/view?usp=share\\_link](https://drive.google.com/file/d/1abCoLPoN80W_N0xPl09FCbCky3hVVV0r/view?usp=share_link), or alternatively <https://youtu.be/6C3WQ1A5pMg>

In the following section, the performances of Horizonist are simulated in terms of settling time and power consumption.

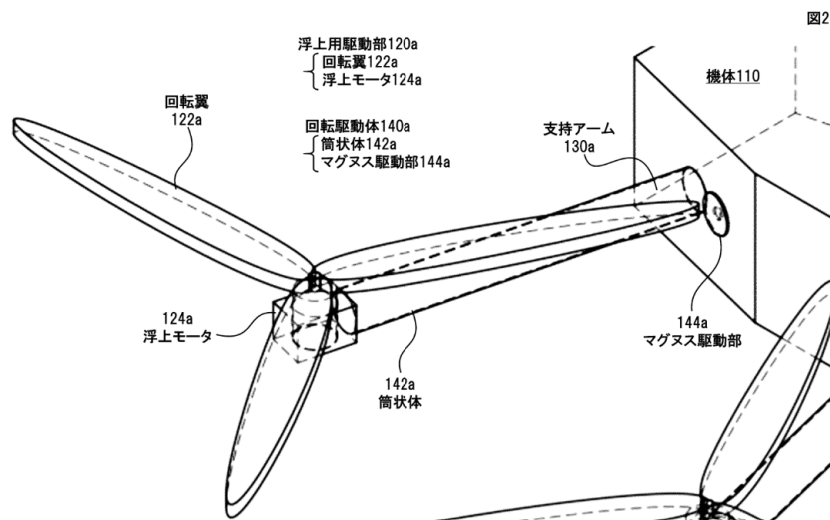


Fig. 1 Blueprint of Horizonist from Japanese Patent Office Information Service [5]

### III. Modelling the system and control design

#### A. The physical model

Modelling an aircraft flight involves some complexity, such as 6 DoF, and the effect of the wind generated by its own propeller. So for the sake of brevity, the following simplifications are made. The model is described in Figure 3.

- 1) The vertical equilibrium is always kept.
- 2) Only horizontal movement in one direction is considered. (i.e., y-axis only)
- 3) The aircraft rotates only on x-axis.
- 4) drag coefficient of the aircraft is constant regardless of the orientation and Reynolds number.
- 5) Actuators are "ideal" and instantaneously reach the bespoke output, and the power efficiency is unity.

#### B. The control design

As mentioned in the previous section, we only consider two degrees of freedom. Therefore, as in Figure 3 variables which are to be controlled are  $\theta$ , the roll of the aircraft, and  $y$ , the location of the aircraft. Both of them are measured from fixed frame of reference.  $i$  and  $j$  are on the frame of the aircraft. Figure 4 represents the control system of the simulation. The aircraft can move horizontally by tilting its body, so the controller changes the output of actuators and applies torque,  $T(s)$ , to adjust the roll angle. In addition to torque applied by actuators, when the Flettner rotors (142a in

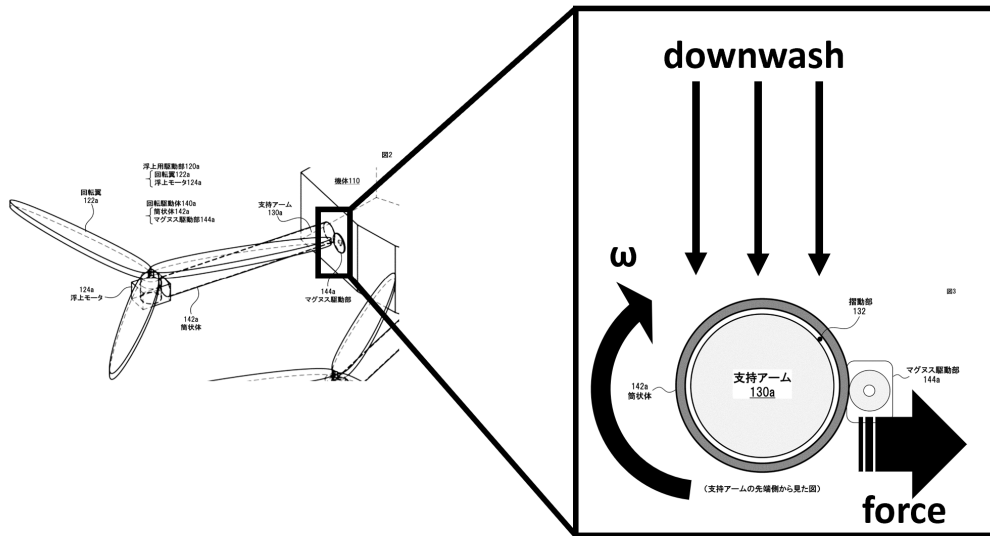


Fig. 2 Detailed schematics of Horizonist

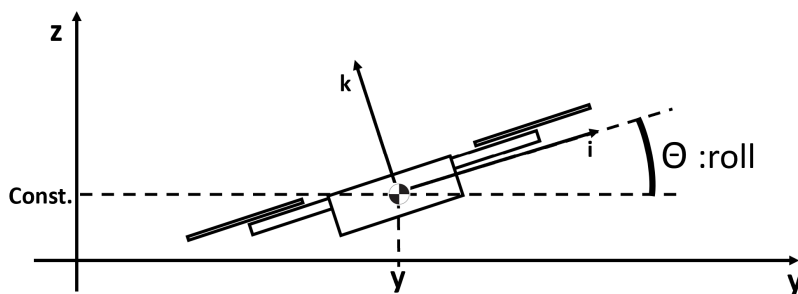
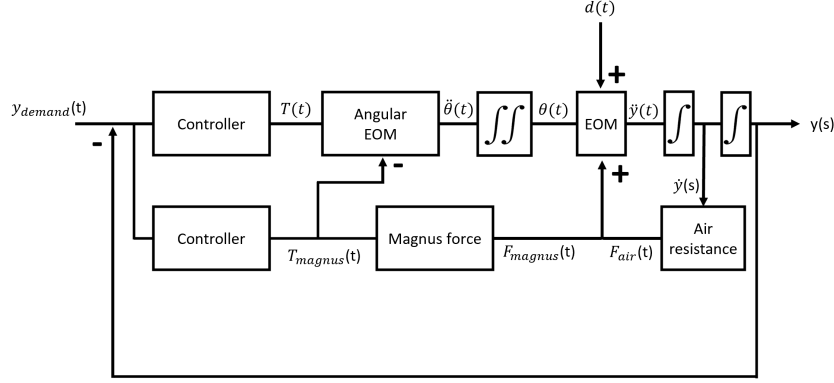


Fig. 3 The physical model of the simulation



**Fig. 4 The block diagram of the control system**

Figure 3) are activated, the anti-torque from the Flettner rotors is applied to the aircraft. This is denoted as  $T_{magnus}$  and therefore the angular equation of motion becomes,

$$\ddot{\theta} = \frac{T + T_{magnus}}{J} \quad (1)$$

By integrating twice, the roll angle is obtained.

$$\theta = \int \int \ddot{\theta} dt dt \quad (2)$$

Now, with tilting and by the virtue of the assumption that the vertical equilibrium is always kept, the thrust in the y direction is,

$$F_{tilt} = -mg \tan \theta. \quad (3)$$

When the Flettner rotors are activated, horizontal thrust is created due to the Magnus effect, and in y direction it is,

$$F_{magnus_y} = F_{magnus} \cos \theta. \quad (4)$$

Note that the vertical component of the Magnus force is neglected. Finally, on the aircraft body the wind is applied due to disturbance and the velocity of the aircraft so, respectively they can be written as

$$F_{disturbance} \quad (5)$$

$$F_{air} = -\text{sign}(\dot{y}) \frac{1}{2} \rho \dot{y}^2 C_d A \quad (6)$$

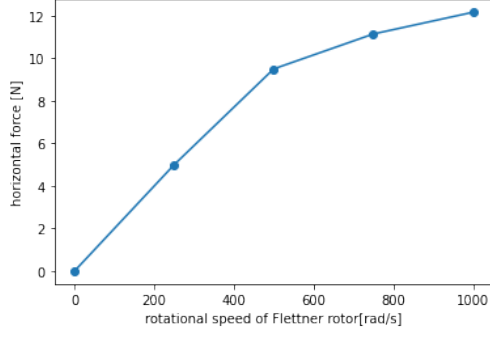
Considering all the forces, the equation of motion about y is

$$EOM : \ddot{y} = -g \tan \theta + \frac{F_{disturbance} + F_{air} + F_{magnus_y}}{m} \quad (7)$$

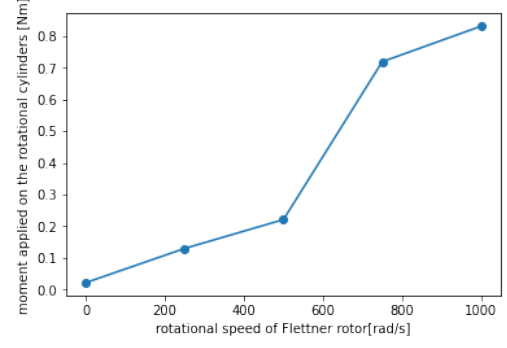
In this paper  $m = 55kg$  and  $J = 9kgm^2$  are used to calculate the performance of the aircraft. This is exactly the same condition as [6].

#### IV. The calculation of the energy consumption

The second simulation is about the comparison of the energy consumption between Hozrizonist and the conventional method. In this series of simulations, a step input, ramp input, and square wave input are tested. Since [6] does not offer a discussion of energy consumption and various input, the author created a conventional PID drone control system as an alternative for the reference. The control system consists of one distance PID whose output is the ideal roll angle and one PID roll angle control unit. The total energy consumption seems to be:



(a) The relationship between the Magnus force and Flettner rotor speed



(b) The relationship between the moment required and Flettner rotor speed

Fig. 5 CFD results

$$[workdone] = \int \mathbf{F} \cdot \mathbf{v} dt \quad (8)$$

However, Equation 8 only represents the energy which is converted to useful mechanical energy. The actual work input is, therefore from [7]:

$$[workinput] = \int \frac{\mathbf{F} \cdot \mathbf{v}}{\mu_{Froude}} dt \quad (9)$$

where  $\mu_{Froude}$  is the Froude efficiency such that:

$$\mu_{Froude} = \frac{2V_{travel}}{V_{jet} + V_{travel}} \quad (10)$$

, and  $V_{jet}V_{travel}$  are respectively the speed of air exhausted from propellers and the speed of the aircraft. For the sake of brevity,  $V_{jet} = 20$  is used and the negligible  $V_{travel}$  is assumed.

The power consumption and the Magnus force of the Flettner rotors are obtained from a CFD simulation software, "FlighStream" from Research In Flight Co. The results are shown in Figure 5. The maximum rotational speed is assumed to be 1000 [rad/s] in this series of experiments, and hence the maximum Magnus force from each unit is 12.15N. For more about the CFD simulation, refer to Appendix VI.B.

## V. Results

### A. The settling time

Figures 7a and 7b are the step responses of the aircraft. The moment inertia of about the rotating axis is  $9kgm^4$ [6]. Figures 8a, 9a and 10a displays the responses of Horizonist, and the conventional drone model made by the author. The fluctuations in the conventional models' response are to be noted. This was unable to be fixed by the author with calibration. Both model are "ideal" and actuator can rotate at bespoken values without any time delay. Furthermore, the response against the wind is also simulated. In the simulation, winged VTOL as in Figure 6 is used. The winged VTOL simulation is motivated by the application as in Appendix in the later section.

### B. The power consumption

Power consumption in the twenty-second time frame for each input and for each model is illustrated in Figures 8b, 9b and 10b. Y-axis for each graph is logarithmic logarithmic.

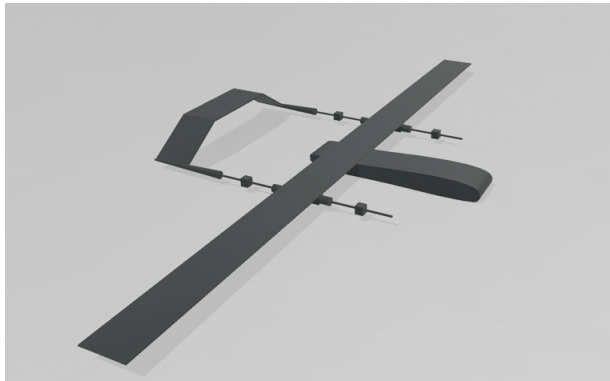
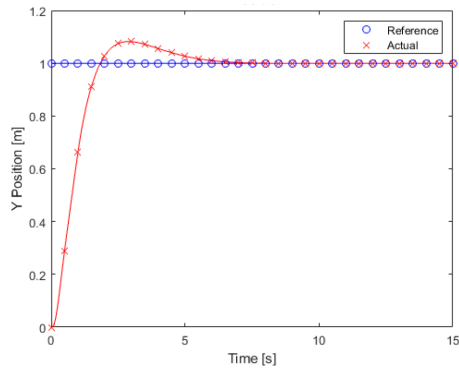
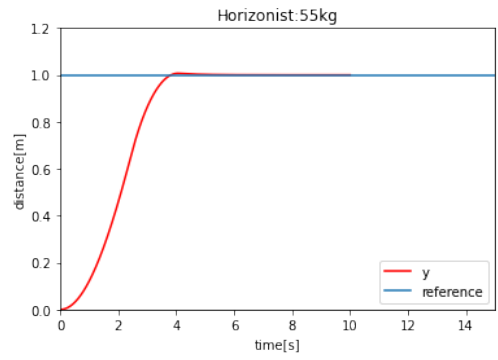


**Fig. 6 Winged drone CAD**

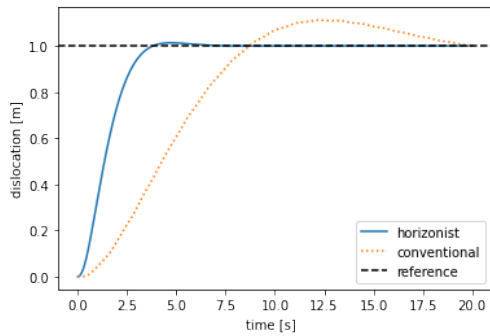


**(a) step response of [6]'s aircraft**

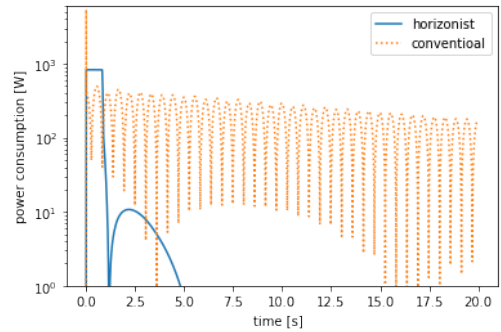


**(b) step response of Horizonist**

**Fig. 7 Simulation results**

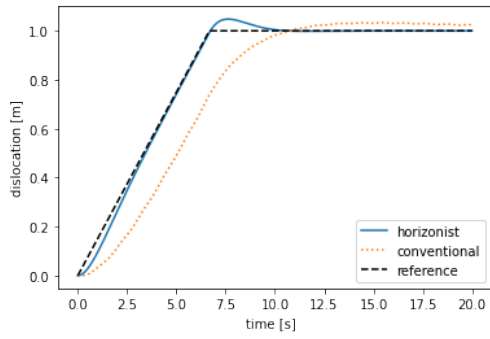


**(a) the dislocation**

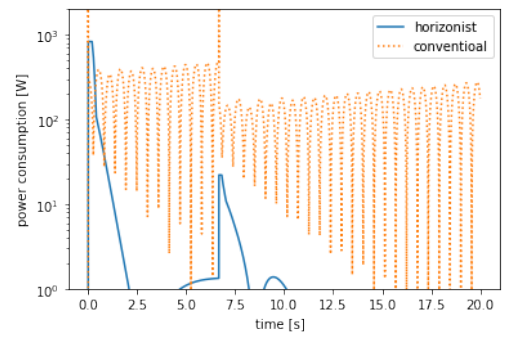


**(b) the power consumption**

**Fig. 8 step responses of idealised Horizonist and the conventional aircraft**

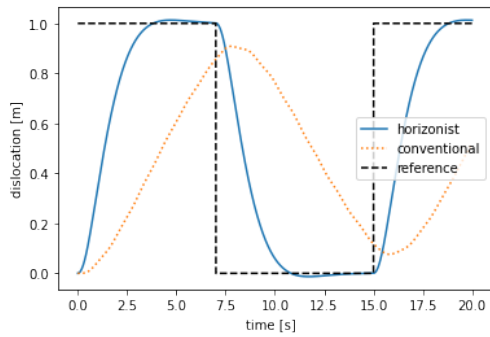


(a) the dislocation

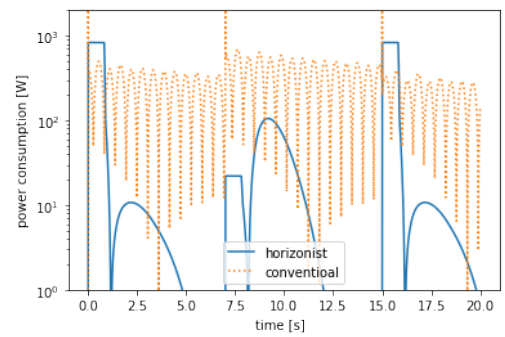


(b) the power consumption

**Fig. 9** lamp responses of idealised Horizonist and the conventional aircraft



(a) the dislocation



(b) the power consumption

**Fig. 10** Square wave responses of idealised Horizonist and the conventional aircraft

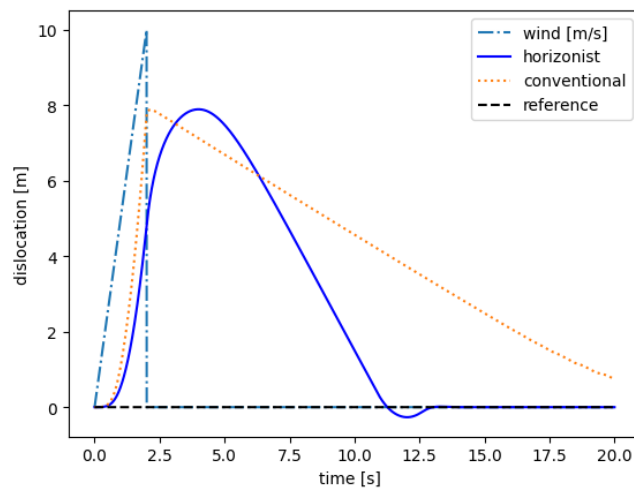


**Fig. 11** wind response of Horizonist and the conventional aircraft

## VI. Discussion

### A. The step response settling time

Comparing the results in Figure 7, it can clearly be seen that Horizonist responds faster than [6] by approximately 2 seconds. No significant overshooting is observed in 7b. From these results, Horizonist is suggested to respond faster than [6] by 33%.

### B. The energy consumption and the responses for various input

Although the instability can be seen in the conventional models, overall trends can still be discussed by looking at Figure 7, 9 and 10. For all three inputs, Horizonist shows quicker, but yet more energy-efficient responses than the conventional. Especially for the square wave input, Horizonist can catch up with the input whereas the conventional does not. Spikes in power consumption are flattened for Horizonist. This makes Horizonist more advantageous because high-voltage electronics are unnecessary for the flight. The first 10 second's energy consumption ratio of the conventional to Horizonist in Figure 8b, 9b, and 10b are 7.93, 8.28, and 7.49 respectively. The power consumption of only the first half was explored in order to reduce the effect of the power consumption caused by the fluctuations which are amplified at a later time and realistically don't exist. Regardless, the first 10 seconds of power consumption results suggest Horizonist's better energy performance. However, the conventional outperforms in terms of the power consumption for the first second for all input types, the step, lamp and square waves.

### C. The wind response

The wind response of both aircraft are compared in Figure 11. Horizonist has faster response overall, but the drafting distances are the same in both types of aircraft at around 8 m. Looking at the time when the aircraft is under the wind, Horizonist is pushed less than the conventional, but the recovery from the wind is clearly inferior to that of the conventional, causing the same drifting distance. Due to the massive wind area, however, the conventional struggles to come back to the reference position, resulting in the slow convergence. From this result, the characteristics that the conventional method has an advantage under low relative air velocity, and that Horizonist performs better in high relative air velocity are confirmed. The optimal control method would be the hybrid of these, and this remains as a future work.

## VII. Conclusion

This paper investigates the performance of the Flettner-rotor-powered VTOLs compared to the conventional ones. The simulations suggest that Horizonist is expected to have very higher agility than the conventional while maintaining lower power consumption. Although these simulations rely on CFD results and the accuracy remains in question, in combination with the PoC video that is mentioned earlier and physical first principles that tilt-less flight saves time to respond, these results may well be said to well represent the performance of Horizonist in contrast to the conventional. Making a drone and measuring response time and power consumption experimentally is the next work to confirm if the Flettner-rotor-powered VTOLs are superior to the conventional or not as well as exploring the possibility of hybrid control system.

## Acknowledgements

Satoki Shimamune thanks Dr Dmitry Ignatyev from Cranfield University for his strategic advice.

## Appendix

### A. application of Horizonist

In this section, application examples of Horizonist are listed. By the virtue of its tilt-less flight, Horizonist is especially suited for winged VTOLs, which have high moment of inertia and cross sectional area when tilted due to their wings. Winged VTOLs are known for its speed and flight range, whereas the stability of their hovering is poor. However, with Horizonist, the stability can greatly improved, while maintaining the speed and flight range. Therefore as displayed in the right of Figure 12, the aircraft can cover wider area from its station (shown in the black dots) and saves costs and labor required for transporting the aircraft itself to the place of interest (shown in the red dots). The followings



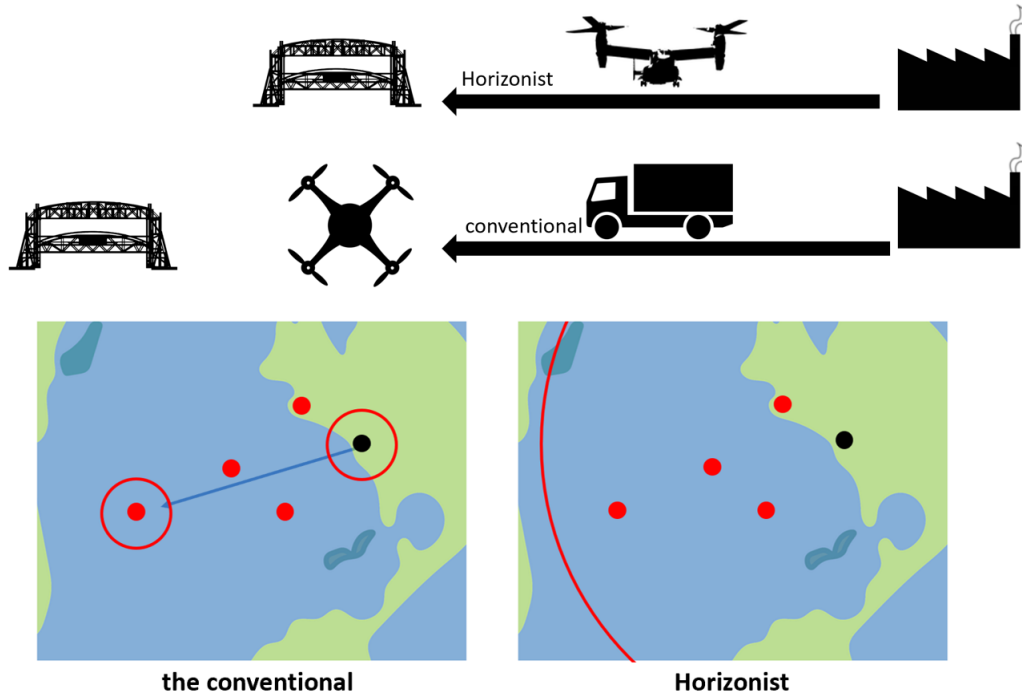


**Fig. 12 An application example of Horizonist**

are the examples.

- 1) Inspection of large infrastructure, such as wind turbines, oil pipes, bridges in the remote area, and power lines.
- 2) Luxurious drone taxis. Tilt-less flight increases the comfort of the flight for the passengers.
- 3) Deployment of anti-submarine dipping sonars.
- 4) Other types of civil/military applications that requires rebustness and stability.

## **B. CFD**

The CFD software, FlightStream from Research In Flight Co., was used to acquire the relationship among the angular velocity of the Flettner rotor, the moment required to sustain the angular velocity, and the Magnus force created at the angular velocity. In the CFD simulation, only one of the four arms is simulated to save the computational expenses. The mesh of the simulation is shown in Figure 13. The green ring in the figure generates flow created by the propeller, which can be activated from "actuator" function in FlightStream. The diameter of the arm is 40mm and there are two rotating surfaces with length of 130mm. Both ends of the arms are fixed geometries. Figure 14 illustrates the schematics of the arm. The 13.00 cm neck sections are covered by the rotating cylinders and the assembly of these three parts looks like Figure 13.

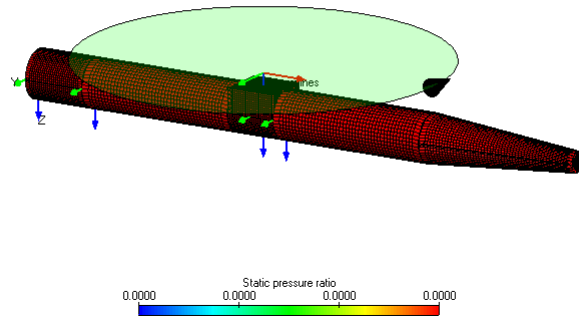


**Fig. 13** CFD mesh

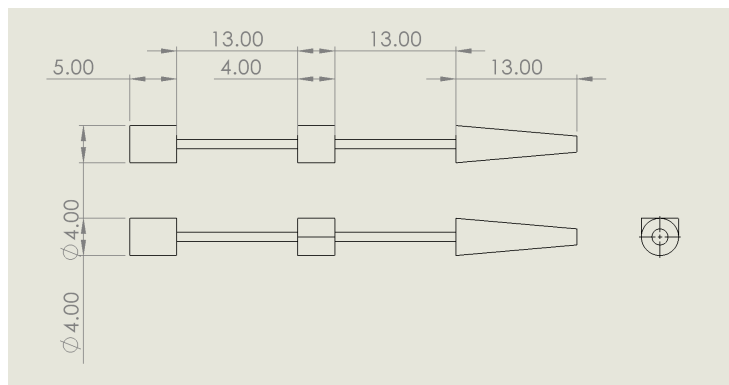


**Fig. 14** Schematics of the arm

## References

- [1] Seifert, J., “A review of the Magnus effect in aeronautics,” *Progress in Aerospace Sciences*, Vol. 55, 2012, pp. 17–45. <https://doi.org/https://doi.org/10.1016/j.paerosci.2012.07.001>, URL <https://www.sciencedirect.com/science/article/pii/S0376042112000656>.
- [2] Giribet, J. I., Sanchez-Pena, R. S., and Ghersin, A. S., “Analysis and design of a tilted rotor hexacopter for fault tolerance,” *IEEE Transactions on Aerospace and Electronic Systems*, Vol. 52, No. 4, 2016, pp. 1555–1567. <https://doi.org/10.1109/TAES.2016.140885>.
- [3] Mousaei, M., Geng, J., Keipour, A., Bai, D., and Scherer, S., “Design, Modeling and Control for a Tilt-rotor VTOL UAV in the Presence of Actuator Failure,” *2022 IEEE/RSJ International Conference on Intelligent Robots and Systems (IROS)*, IEEE, 2022. <https://doi.org/10.1109/iros47612.2022.9981806>.
- [4] Muraoka, K., Okada, N., and Kubo, D., “Quad Tilt Wing VTOL UAV: Aerodynamic Characteristics and Prototype Flight,” 2009. <https://doi.org/10.2514/6.2009-1834>.
- [5] Shimamune, S., “The flight systems and flight control program,” *Japan Patent Office*, , No. P6938005, 2021.
- [6] Türkmen, A., and Altuğ, E., “Design of a Quad-Jet VTOL UAS for Heavy-lift Applications,” *ICUAS*, Vol. 24, No. 11, 2020, p. 875. <https://doi.org/https://doi.org/10.1109/ICUAS48674.2020.9214047>.
- [7] N.A. Cumpsty, G. P., C.A. Hall, *the design of the engines for a new large aircraft*, Cambridge University Engineering Department, 2014.

2023-06-08

# Flettner-rotor-powered VTOL s theoretical performances

Shimamune, Satoki

AIAA

---

Shimamune S, Ignatyev D. (2023) Flettner-rotor-powered VTOL s theoret

2023 AIAA Aviation and Aeronautics Forum and Exposition (AIAA AVIATION Forum), 12-16

June 2023, San Diego, USA

<https://doi.org/10.2514/6.2023-4283>

*Downloaded from Cranfield Library Services E-Repository*